Regular Article

PHYSICAL CHEMISTRY RESEARCH
Published by the
Iranian Chemical Society
www.physchemres.org
info@physchemres.org

Phys. Chem. Res., *Vol. 3, No. 3, 239-245, September 2015.*
DOI: 10.22036/pcr.2015.10137

Amphiphilic Block Copolymer Nano-micelles: Effect of Length Ratio of the Hydrophilic Block

N. Nikoofard* and F. Maghsoodi
Institute of Nanoscience and Nanotechnology, University of Kashan, Kashan 51167-87317, Iran
(Received 30 April 2015, Accepted 7 July 2015)

Block copolymer nano-micelles are especially important in cancer treatment because of their fine dimensions. In this article, three systems of amphiphilic copolymers with similar lengths and different ratios of the hydrophobic and hydrophilic chains are studied using implicit-solvent coarse-grained molecular dynamics simulations. The factor f_{phil} is defined as the ratio of the number of hydrophilic monomers to the total number of monomers. Three different values are examined $f_{phil} = 0.65$, $f_{phil} = 0.55$ and $f_{phil} = 0.40$. The time evolution and the final shape of the assembled nano-structures are investigated. The shapes of the nano-micelles are symmetric in the two larger hydrophilic ratios. However, the nano-micelle becomes asymmetric in the one smaller hydrophilic ratio. The average diameters of the whole nano-micelle and its hydrophobic core are calculated. These diameters are obtained by direct calculation from the particles coordinates and by using the radial distribution functions. The sizes of the nano-micelles and their stabilities increase considerably with decreasing the length of the hydrophilic chain. Correspondence of the results on the geometry, size and stability of the nano-micelles with the experimental findings is discussed.

Keywords: Amphiphiles, Copolymers, Nano-micelles, Implicit-solvent simulation, Cancer treatment

INTRODUCTION

Amphiphilic block copolymers are composed of hydrophilic and hydrophobic blocks. Because of the simultaneous presence of hydrophilic and hydrophobic properties, these molecules are organized into nano-structures. The hydrophilic and hydrophobic blocks construct the shell and the core of the nano-structures, respectively [1]. Block copolymer amphiphiles have been a subject of interest for many years because of their diverse applications [2,3,4]. Specifically, amphiphilic block copolymer nano-micelles have an uncharged yet water-soluble shell besides a size in the range of 10-100 nm, which decreases their interruption by the immune system and increases their penetration into cancerous tissues [5,6]. They are also of general interest as drug carriers and different approaches are being explored to enhance their stability [7].

*Corresponding author. E-mail: nikoofard@kashanu.ac.ir

Three main morphologies are observed for amphiphilic copolymers with decreasing the length of the hydrophilic block; spherical and cylindrical micelles and bilayers [8]. Three factors govern the equilibrium formation of the nano-structures from amphiphilic copolymers: (1) the interfacial tension of the core, (2) the entropic repulsion between the hydrophilic blocks in the shell and (3) the entropic cost of stretching the hydrophobic chains in the core [2]. As the hydrophilic blocks become smaller, the entropic repulsion between the chains comprising the shell decreases and the assembly adopts a smaller curvature (Fig. 1). As a result, a transition from spherical to cylindrical micelles is observed by decreasing the hydrophilic ratio of the amphiphilic polymers [8].

It is observed experimentally that increasing the length of the hydrophobic blocks -in a fixed length for the hydrophilic block-leads to a larger number of polymers in each micelle. The larger number of aggregated polymers in a micelle is a result of the tendency to decrease the interfacial tension of the core. The size of the micelle

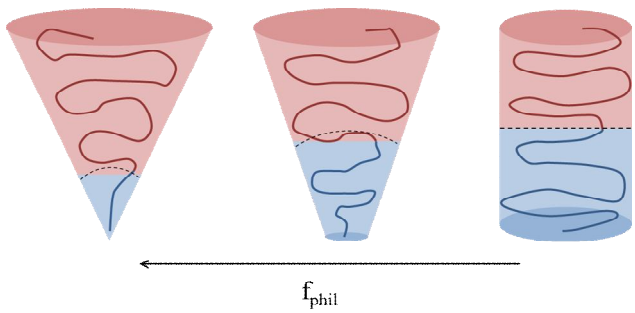

Fig. 1. Effect of the hydrophilic ratio of the diblock copolymer on the final morphology of the nano-structure. The conformation of copolymer in the self-assemblies is shown. Blue and red regions correspond to the core and the shell of the nanostructure, respectively. Decreasing the length of the hydrophilic block decreases the entropic repulsion between the shell-forming chains. So, the nano-structure adopts a lower curvature with decreasing the hydrophilic ratio [2]. The dashed lines show the core curvature.

increases with the length of the hydrophobic blocks. The size of the shell also increases slightly because of the dense packing and so the stretching of the chains in the shell [9].

Increasing the size of the hydrophobic block can lead to an increase in the micelle stability. This can be explained considering the fact that escape of a polymer from a micelle is accompanied by passing through an energy barrier. For micelles with larger cores, this barrier is higher and the polymers can escape from the micelles rarely [10].

Alongside experiments, atomistic and coarse-grained computer simulations have been used to reveal the mechanism of formation of the self-assemblies from amphiphiles, details of the final nano-structures, and their different properties [11-15]. Coarse-grained simulations are becoming a popular tool in the study of biopolymers [15]. They are used to overcome the limitations on the time and length-scale of atomistic simulations. The computational cost is reduced by grouping several atoms into effective interaction sites [16,17].

Coarse-grained models do not contain detailed properties of the solvent molecules and so the hydrophobic effect. In these models, the solvent molecules are just used to enforce the attraction between the hydrophobic parts, at a high computational cost. As a result, many works have used the alternative way of applying an effective attractive potential between the hydrophobic monomers. Implicit-solvent models are common in polymer physics and are shown to be successful in generating the self-assembly of lipid membranes and their physical properties [18-20]. These models are also used in the simulation of the self-assembly of copolymer micelles [21,22].

In this manuscript, we use implicit-solvent coarse-grained molecular dynamics simulations to study the aggregation of block copolymer amphiphiles into nano-micelles. To investigate the effect of changing the length of the hydrophilic and hydrophobic chains on the final structure, the factor f_{phil} is defined;

$$f_{phil} = \frac{N_{phil}}{N_{phil} + N_{phob}} \tag{1}$$

Here, N_{phil} and N_{phob} are the number of monomers of the hydrophilic and the hydrophobic blocks, respectively. In our simulations, this factor is considered to have three different values: f_{phil} = 65%, f_{phil} = 50% and f_{phil} = 40%. In each case, the time evolution of the system and the final structure of the self-assemblies are investigated. Notably, very different results are observed for the three mentioned regimes. Decreasing the hydrophilic ratio of the amphiphilic polymers, the size of the self-assembled nano-structures increases considerably. Also, a smaller hydrophilic length ratio leads to a much higher stability for the self-assembly. In the lowest examined hydrophilic ratio, a transition from spherical to cylindrical micelle is observed. The obtained results are in agreement with experimental findings. This shows that implicit-solvent models are useful in the investigations of the properties of the micelles.

SIMULATION METHOD

Preparation of the Simulation Box

Extensible Simulation Package for Research on Soft Matter (ESPResSo) is used for performing the simulations [23]. The results are visualized using VMD [24]. The simulation box is taken to be 100σ in each dimension (σ is the size of a monomer and the length scale of the

simulations). 200 amphiphilic polymers each with 20 monomers are entered into the simulation box. Periodic boundary conditions are applied in three dimensions. The temperature of the system is fixed at the room temperature using the Langevin thermostat [25].

Three different length ratios of the hydrophilic and the hydrophobic blocks are investigated. Note that total number of the monomers of each polymer is constant.

(1) f_{phil} = 65%, N_{phil} = 13, N_{phob} = 7

(2) f_{phil} = 50%, N_{phil} = 10, N_{phob} = 10

(3) f_{phil} = 40%, N_{phil} = 8, N_{phob} = 12

At the beginning of the simulations, the monomers of each polymer are arranged on a line. Two layers of polymers with their hydrophobic blocks opposite to each other are arranged on the sites of a cubic lattice. The lattice spacing and the distance between the two polymer layers are equal to 2σ and σ, respectively. This arrangement is chosen to speed up the initial aggregation of the molecules into micelles.

Force Fields

The solvent molecules are not considered explicitly in the simulations. Instead, their effect on the hydrophobic monomers is considered through an effective attraction between these monomers. The Lennard-Jones potential with an attraction well is used to effectively include the interaction between the hydrophobic monomers;

$$V_{LJ}(r) = 4\varepsilon\left((\frac{\sigma}{r})^{12} - (\frac{\sigma}{r})^{6}\right) \quad (2)$$

The cut-off radius is taken equal to 20σ. ε and σ are the depth of the attraction well and the size of the monomers, respectively. These are taken as the energy and length units, so the simulations are performed in reduced units.

The hydrophilic monomers do not have attraction with each other and with the hydrophobic monomers. The attraction well between these monomers is eliminated by cutting and shifting the Lennard-Jones potential, at the minimum. The shifted-truncated Lennard-Jones potential with a cut-off radius of $\sqrt[6]{2}\sigma$ is used between the hydrophilic and hydrophobic monomers and between the hydrophilic monomers;

$$V_{LJ}(r) = 4\varepsilon\left((\frac{\sigma}{r})^{12} - (\frac{\sigma}{r})^{6} + \frac{1}{4}\right) \quad (3)$$

If ε and σ are different for each of the hydrophobic and the hydrophilic monomers, then ε and σ between hydrophobic and hydrophilic monomers should be calculated using the relations; $\sigma_{phil/phob} = (\sigma_{phil} + \sigma_{phob})/2$ and $\varepsilon_{phil/phob} = (\varepsilon_{phil} + \varepsilon_{phob})/2$. However, it is assumed here that ε and σ are similar for hydrophobic and hydrophilic monomers. The potentials used between all possible pairs of monomers are given in Fig. 2.

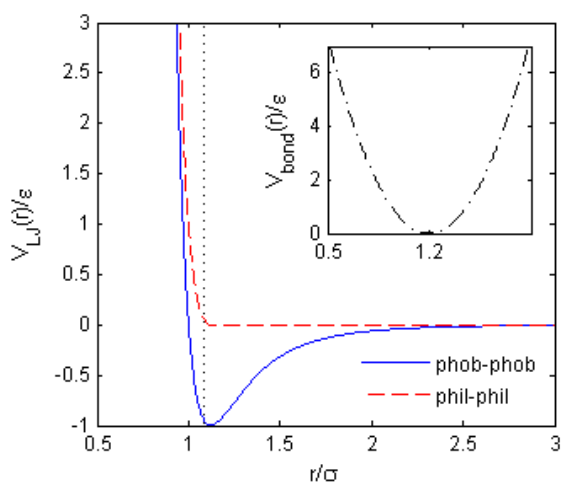

Fig. 2. Lennard-Jones potential between different sets of monomers. The blue solid line is the Lennard-Jones potential with an attraction well between the hydrophobic monomers. The red dashed line corresponds to the shifted-truncated Lennard-Jones potential between hydrophilic monomers. The same potential is used between hydrophobic and hydrophilic monomers. The dotted vertical line shows the position of the minimum of the Lennard-ones potential, which is also the cut-off radius for the shifted-truncated Lennard-Jones potential. Inset: The harmonic potential between adjacent monomers of the polymer.

Since the simulations are performed in reduced units, the present results are applicable for any amphiphilic polymer that the Lennard-Jones parameters for its hydrophilic and hydrophobic monomers are similar.

Adjacent beads of each polymer are bonded to each other via the harmonic potential;

$$V_{bond}(r) = \frac{1}{2}K(r-R)^2 \tag{4}$$

The spring constant and the equilibrium length of the harmonic potential are taken equal to $30\varepsilon/\sigma^2$ and 1.2σ, respectively (Inset of Fig. 2). No bond angle potential is defined between the monomers and the amphiphilic polymers are assumed to be flexible. Also, the polymers are taken uncharged.

Integration and Calculations

The Langevin equation is integrated to find the time evolution of the position of each monomer;

$$m\frac{d\upsilon(t)}{dt} = F(t) - \gamma m\upsilon(t) + \xi(t) \tag{5}$$

Here, m and $v(t)$ are the mass and velocity of the monomer, respectively. $F(t)$ is the force from the rest of monomers. The effect of the solvent is included in the two terms: $-\gamma mv(t)$ and $\zeta(t)$; the friction and the random force from the solvent respectively. The random force mimics collisions with the solvent molecules and is a Gaussian white noise. The step size is taken equal to 0.01 times the simulation time unit. The time unit of the simulation is given by the relation

$$\tau = \sqrt{\frac{m\sigma^2}{\varepsilon}} \tag{6}$$

The integration is continued for 100,000 time units (10^7 time steps). We find the mean diameters of the micelles and their cores from the final step of the simulation. Two different methods are used to find the mean diameters:

(1) The positions of the hydrophobic and the hydrophilic monomers are directly used to find the diameters. Averaging in different directions is used to find the mean diameter of the symmetric micelles.

(2) The radial distribution functions (RDF) of the hydrophilic and hydrophobic monomers are calculated. The first RDF describes the total size of the micelles, while the second one gives the size of their cores. The distance at which the RDFs become zero is equal to the diameter of the corresponding structure.

It is observed that the diameters obtained from the two methods are very close to each other. This confirms that both methods are suitable for calculating the size of nano-structures in computer simulations.

RESULTS AND DISCUSSION

f_{phil} = 65%

At the beginning of the simulation, the initial structure divides into four primary micelles, which lose many polymers over time. Three of the micelles become nearly stable and no polymer is removed from them after times 52000, 69000 and 84000 (in simulation units). The fourth micelle loses most of its polymers up to the time 94,000. This micelle is supposed to be an out-of-equilibrium structure and is not considered in calculations. Finally, three stable small micelles and many single molecules are present in the main simulation box (Fig. 3a). The number of polymers in the stable micelles -equal to 34, 34 and 43- is unchanged at least in the last 16,000 time units of the simulation. These micelles are supposed to be in equilibrium and their sizes are measured in the final step of the simulation.

Using the particle coordinates, the mean diameters of the three micelles are found to be 22.22, 19.2, and 19.76 (with an average equal to 20.39). The same method gives the mean diameter of their cores equal to 10.2.

Radial distribution functions of the hydrophobic and the hydrophilic monomers are shown in Fig. 4a. The RDF of the hydrophobic monomers becomes zero at the distance 10. This number is in agreement with the mean diameter of the micelle cores, obtained by direct use of the particle positions. The RDF of the hydrophilic monomers becomes zero at distance 20, which gives the mean diameter of the micelles. It is close to the average value of the micelle size obtained from the particle coordinates.

f_{phil} = 50%

At the beginning of the simulation, the whole polymers

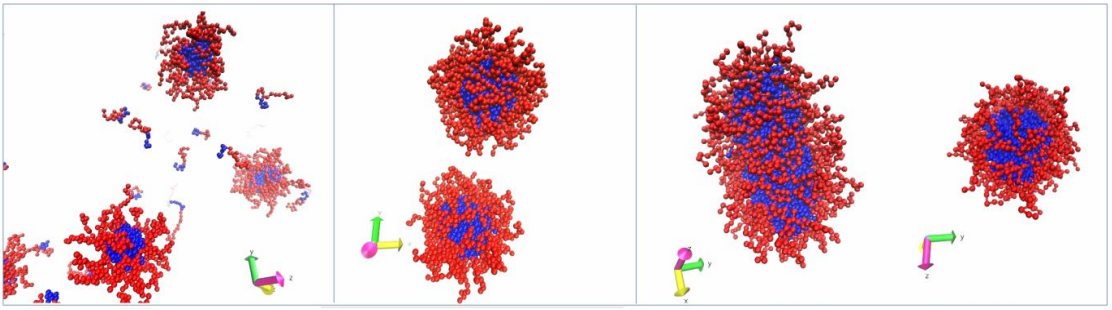

Fig. 3. Schematics of the simulation results for the three hydrophilic ratios. The hydrophobic and hydrophilic monomers construct the core and the shell of the micelles, respectively. (a) f_{phil} = 65%: There are three micelles and many single molecules in the solution. (b) f_{phil} = 50%: There are only one single molecules in the simulation box, which do not take part in the micelles structure (not shown here). (c) f_{phil} = 40%: The final structure is shown along two different axis.

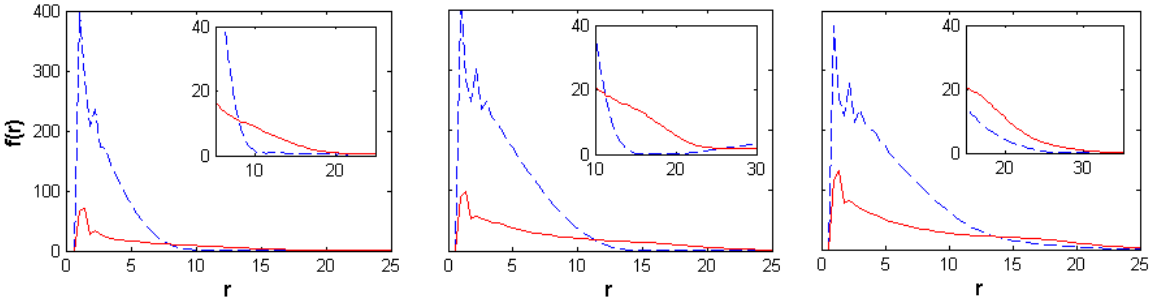

Fig. 2. Radial distribution functions. The red solid lines and the blue dashed lines correspond to the RDFs of the hydrophilic and the hydrophobic monomers, respectively. The distances at which the RDFs become zero are used to find the diameters of the micelles and their cores. The RDF tails are magnified in the insets to show the positions at which the functions become zero. (a) f_{phil} = 65%. (b) f_{phil} = 50%. (c) f_{phil} = 40%.

(except one) form a single micelle. This micelle elongates over time and divides into two smaller micelles. The shape and the size of the two micelles and their distance become constant after 14,000 simulation time units. The system remains unchanged for the rest of the simulation, indicating that the system has reached to equilibrium. Finally, there is one solitary polymer in the simulation box and all other molecules take part in the micelles (Fig. 3b). The number of polymers in the two final micelles is equal to 105 and 94 polymers.

The constant distance between the micelles is a result of attraction between the hydrophobic cores of the micelles. Although attraction between each pair of the hydrophobic monomers is very small in such a distance, the total attraction between the cores becomes considerable. It seems that the steric repulsion arisen from the polymeric shell of the micelles resists the complete absorption of the micelles into each other.

The mean diameters of the two micelles in the y-z plane are 25.39 and 23.93. In the x-y plane, the mean diameters of the same micelles are 25.04 and 25.55. These measurements show that the structures are nearly symmetric. The mean diameters of the cores are 15.2 and 13.04. As a result, the mean diameters of the whole micelles and their cores are

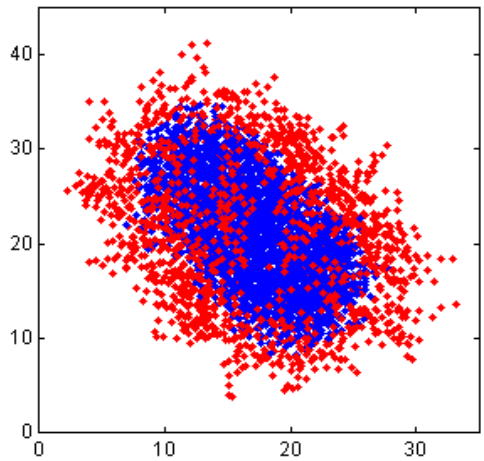

Fig. 3. Position distribution of the monomers in the nano-micelle. Hydrophilic and hydrophobic monomers are shown with red and blue dots, respectively. The hydrophobic monomers are packed in the core. However, the hydrophilic monomers are extended freely in the shell.

25.22 and 14.13, respectively.

The values of the RDFs of the hydrophilic and the hydrophobic monomers become zero at the distances of 25 and 14, respectively (Fig. 4b). These numbers are very close to the mean diameter of the micelles and their cores obtained above.

f_{phil} = 40%

At the beginning of the simulation, a large micelle containing the whole polymers is formed. This micelle changes shape between a spherical symmetric micelle and an asymmetric cylindrical micelle, repeatedly. The changes happen over a time scale of the order of 1000 time units. A final cylindrical micelle (with a smaller asymmetry relative to previous cylindrical micelles) is formed in the time unit 60000, which is stable in the rest of the simulation (Fig. 3c). Considering that the final micelle is stable over nearly half of the simulation time, it can be regarded as an equilibrium structure. The micelle contains all of the 200 monomers and there is no single molecule in the system.

The mean height of this nano-cylinder is equal to 31.19. The mean diameters of the cross section along the two orthogonal axes are 25.58 and 21.97. The mean height of the hydrophobic core is 25.7, while the mean diameters of the core cross section along the same axes are 17.17 and 15.79.

Radial distribution functions of the hydrophilic and the hydrophobic monomers become zero at the distances 31 and 25 (Fig. 4c). These numbers are close to the heights of the whole structure and its core, respectively.

It should be noted that in all simulations, the monomers in the hydrophobic core are packed in a globular structure. However, the monomers in the hydrophilic shell are extended freely in the solution (Fig. 5). This is in agreement with the results obtained in Ref. [26].

CONCLUSIONS

Implicit-solvent coarse-grained simulations were performed on the self-assembly of amphiphilic copolymers. It was shown that when the length ratio of the hydrophilic block is equal to 65%, small spherical nano-micelles with low stability are formed in the solution. In this condition, many of the amphiphilic molecules diffuse solitary in the simulation box. In equal lengths for the hydrophilic and the hydrophobic blocks, the molecules are still organized into symmetric spherical nano-micelles, but with higher sizes and stabilities. In the smallest length ratio of the hydrophilic block, all molecules form a single large cylindrical micelle.

Different geometries of the nano-micelles from block copolymers can be understood by a simple explanation, considering the entropy of the hydrophilic block [2,3]. A more curved structure of the micelle provides a wider space for the fluctuation of the extended hydrophilic blocks. A cylindrical nano-micelle has a lower curvature relative to a spherical nano-micelle. Thus, the geometry is changed from spherical to cylindrical when the hydrophilic ratio is decreased. This change in the morphology of the nano-structure is also reported experimentally (Section 3.3.1 of Ref. [2]).

Larger size of the nano-micelles with increasing the hydrophobic ratio is somewhat trivial, considering the larger energy gain of the molecules upon aggregation. It is also shown experimentally that the number of polymers belonging to each micelle and the size of the micelles increase with the length of the hydrophobic block [9].

Higher stability of the nano-micelles is observed by a small change in the length of the hydrophobic block. The stability of the micelles is related to the rate of polymer escape from a micelle. It is also shown experimentally that the escape rate of the polymers is highly sensitive to the core chain length [10].

To map the simulation results to the experimental ones, the coarse-grained monomers should be defined according to the polymer of interest [27,28]. Consider the case that the coarse-grained monomers are approximately similar to PEG in size. Then, the size unit is replaced by $\sigma = 0.451$ nm [27]. The concentration of the polymers in the solution is obtained around 3.6 mM (200 molecules in a cubic box with the length 100σ). The characteristic sizes of the micelles in the three studied cases were 20.39σ, 25.22σ and 31.19σ. Using the mentioned values for σ, the micelles are found to have the sizes 9.19 nm, 11.37 nm and 14.07 nm, in real units.

A computational result of this article was to show the ability of implicit-solvent models to reproduce the experimental results on copolymer micelles. It was also shown that the mean diameters of the micelles and their cores can be found from the RDFs of the hydrophilic and the hydrophobic monomers, respectively.

REFERENCES

[1] R.L.A. Jones, Soft Condensed Matter, Oxford University Press, Oxford, 2002.

[2] Y. Mai, A. Eisenberg, Chem. Soc. Rev. 41 (2012) 5969.

[3] A. Blanazs, S.P. Armes, A.J. Ryan, Macromol. Rapid Commun. 30 (2009) 267.

[4] A.P. Nowak, V. Breedveld, L. Pakstis, B. Ozbas, D.J. Pine, D. Pochan, T.J. Deming, Nature. 417 (2002) 424.

[5] G. Gaucher, M.H. Dufresne, V.P. Sant, N. Kang, D. Maysinger, J.C. Leroux, J. Controlled Release 109 (2005) 169.

[6] L. Tang, *et al.*, Proc. Natl. Acad. Sci. USA 111 (2014) 15344.

[7] A. Rösler, G.W.M. Vandermeulen, H.-A. Klok, Advanced Drug Delivery Reviews. 64 (2012) 270.

[8] S. Jain, F. S. Bates. Science. 300 (2003) 460.

[9] T. Zinn, L. Willner, R. Lund, V. Pipich, M.S. Appavou, D. Richter, Soft Matter 10 (2014) 5212.

[10] S.H. Choi, T.P. Lodge, F.S. Bates, Phys. Rev. Lett. 104 (2010) 047802.

[11] N. Thota, Z. Luo, Z. Hu, J. Jiang, J. Phys. Chem B 117 (2013) 9690.

[12] O.-S. Lee, S.I. Stupp, G.C. Schatz, J. Am. Chem. Soc. 133 (2011) 3677.

[13] O.-S. Lee, V. Cho, G.C. Schatz, Nano. Lett. 12 (2012) 4907.

[14] Y.S. Velichko, S.I. Stupp, M.O. de la Cruz, J. Phys. Chem. B 112 (2008) 2326.

[15] S. Takada, Current Opinion in Structural Biology 22 (2012) 130.

[16] G. Srinivas, D.E. Discher, M.L. Klein, Nature Materials 3 (2004) 638.

[17] V. Ortiz, S.O. Nielsen, M.L. Klein, D.E. Discher, Polymer Science 44 (2006) 1907.

[18] G. Brannigan, P.F. Philips, F.L.H. Brown, Phys. Rev. E 72 (2005) 011506.

[19] G. Illya, M. Deserno, Biophys. J. 95 (2008) 4163.

[20] B.J. Reynwar, G. Illya, V.A. Harmandaris, M.M. Müller, K. Kremer, M. Deserno, Nature 447 (2007) 461.

[21] A. Milchev, A. Bhattacharya, K. Binder, Macromolecules 34 (2001) 1881.

[22] G.K. Bourov, A. Bhattacharya, J. Chem. Phys. 127 (2007) 244905.

[23] H.J. Limbach, A. Arnold, B.A. Mann, C. Holm, Comput. Phys. Commun. 174 (2006) 704.

[24] W. Humphrey, A. Dalke, K. Schulten, J. Molec. Graphics 14 (1996) 33.

[25] N. Goga, A.J. Rzepiela, A.H. de Vries, S.J. Marrink, H.J.C. Berendsen, J. Chem. Theory Comput. 8 (2012) 3637.

[26] R. Lund, *et al.*, Phys. Rev. Lett. 102 (2009) 188301.

[27] W. Shinoda, R. DeVane, M.L. Klein, Molecular Simulation 33 (2007) 27.

[28] R. DeVane, W. Shinoda, P.B. Moore, M. Klein, J. Chem. Theory Comput. 5 (2009) 2115.